Article

X-ray Diffraction Analysis of Clay Particles in Ancient Baekje Black Pottery: Indicator of the Firing Parameters

Dong-Hyeok Moon [1], So-Jin Kim [1], Sang-Won Nam [2] and Hyen-Goo Cho [3],*

1 Conservation Science Division, National Research Institute of Cultural Heritage, Daejeon 34122, Korea; moondh@korea.kr (D.-H.M.); Kimsj84@korea.kr (S.-J.K.)
2 Research Division of Archaeology, National Research Institute of Cultural Heritage, Daejeon 34122, Korea; nsw918@korea.kr
3 Department of Geology and Research Institute of Natural Science, Gyeongsang National University, Jinju 52828, Korea
* Correspondence: hgcho@gnu.ac.kr

Abstract: An X-ray diffraction (XRD) analysis was conducted after separating clay particles from three shards, to analyze the production technique of black pottery excavated from a historical site of ancient Baekje in Seoul, South Korea. Through the analysis, clay minerals and iron oxides that were not recognized in the XRD patterns of the bulk powder samples were identified. A pottery type with a blackened portion from the surface to the margin and the core was estimated to have been produced in a reduction firing environment of less than 900 °C, by detecting illite and magnetite. As for the other blackened pottery, a brown soil color remained in the core, and the presence of illite and kaolin was confirmed. In addition, while magnetite was detected on the black surface and margin, hematite was detected in the core. These results confirm that this type of blackened pottery was produced through reduction firing at a temperature below 550 °C. In particular, the results indicate that there is a new category of pottery, produced by firing at lower temperatures in a reduction atmosphere, previously not reported by research on ancient Baekje black pottery, which could be discovered due to its specific clay particles.

Keywords: clay particle; clay mineral; iron oxide; ancient Baekje; black pottery; manufacturing technique; firing condition

1. Introduction

Pottery is one of the three elements of the Neolithic Revolution, along with ground stone and the beginning of agriculture. It has evolved in technology, roles, and esthetics over time, and carries various types of information that can be used to estimate the era and living conditions of the historical sites from which it has been excavated. The shape, decoration, and color of pottery, and the mineral and chemical properties of the raw materials used, serve as useful indicators for understanding the cultural and technical levels practiced when the pottery was produced.

Among the various types of pottery, black pottery—with its vivid color and smooth luster, manifested through surface polishing—is one of the commonly unearthed types in ancient sites worldwide. In addition to its artistic and archeological value, this type of pottery is important evidence that ancient people used scientific techniques to materialize the black color. Black pottery is classified into the following three types based on the production techniques and materials used for color development: the black smoked (BS) type, which is produced by a firing technique that allows carbon-based black material, such as soot, to deposit on the surface and penetrate the interiors [1–4]; the black painted (BP) type, in which a carbon, Mn oxide, or reduced iron-based black material is directly painted, with an adhesive, onto the surface of the pottery [5–11]; the reduced black (RB) type, in which the color development takes place due to an increase in the percentage of

Fe^{2+} and magnetite converted from iron oxides in the raw material soil, through reduction firing [12–21]. The specific classification of pottery into the above three types requires precise identification of the minerals used for color development and their chemical compositions. In particular, in the case of the RB type, evaluating the mineralogical factors used for color development, based on the major mineral and element compositions, is sometimes difficult. Consequently, previous studies have made use of Mössbauer spectroscopy [12–15], X-ray absorption near-edge structure [20–24], and an electron energy-loss spectroscopy instrument attached to a transmission electron microscope [25,26], through which the iron oxide composition or the iron oxidation status can be verified.

Various types of black pottery have also been unearthed in South Korea. Among them, the black pottery excavated from the Hanseong period site of the ancient Baekje located in Seoul is a prime example, and studies have been conducted to investigate the mineralogical factors involved in its production. Based on the mineral composition of quartz, feldspar, and mica, detected in various samples, the firing temperature of Baekje black pottery was estimated to be in the range of 700–900 °C [27,28]. Research on blackening techniques has suggested that reduction firing may have been performed after applying a thick coat of iron oxide [29]; however, magnetite was not detected in the scientific analysis conducted later [27,28]. Meanwhile, black pottery with traces of lacquer-containing carbon components in the black part of the surface has been reported to be the BP type [30]. In addition, the type without the lacquer trace was reported to be the BS type [28], based on the presence of carbon detected on the surface of Baekje black pottery and the application of the technique of firing with vegetable fuels to restore the production research conducted in the field of Korean archeology [31–35]. However, the possibility of the RB type existing among ancient Baekje black pottery has been indicated through a recently conducted study on iron oxide compositions using Mössbauer spectroscopy, and the carbon content of the surface and cores [36].

All of the above studies on the mineral composition of ancient Baekje black pottery analyzed the bulk powder collected from pottery fragments and did not examine clay-sized particles containing minerals of small traces or weak crystallinity, such as clay minerals and iron oxides. Many geological studies have used concentrated specimens, by separating and collecting clay particles, to identify the exact composition of clay minerals in the specimens, which is difficult to identify in bulk powder [37–40]. In the case of pottery, the composition of iron oxides and clay minerals that were not detected in the bulk powder must be investigated through mineralogical research on clay particles, as clay-rich soil is the main raw material used.

This study was the first to separate clay particles in black pottery powder unearthed from the archaeological site of ancient Baekje, to identify the clay minerals and iron oxides detected on the surface and in the core of the black pottery for each type. In addition, based on the results, the firing parameters (such as temperature and atmospheric conditions) of the black pottery unearthed from the site were analyzed, and the existence of RB-type pottery was checked.

2. Materials and Methods

2.1. Materials

Three black pottery fragments unearthed from Pungnaptoseong—a historical site of the Baekje Hanseong period (270 to 475 AD), a prime period of Baekje among ancient Korean peninsula nations—were the subject of this study (Figure 1). These samples were the same as those used in an author's previous study using Mössbauer spectroscopy [36]. Fragment PN1 shows a black or grayish black color in the direction from the surface to the core. Furthermore, in PN2, a brownish soil color remains in the core, while a blackened margin part has been formed in the direction from the surface to the interior. Finally, fragment PN3 is a BS type of pottery covered with soot, and it was used as the baseline for distinguishing the properties of this type from those of the RB type.

Figure 1. Pottery shard samples unearthed from the Pungnaptoseong site [36].

2.2. Methods

To examine the surface and inner parts of the pottery specimens, cross-sectional samples, which were polished after cutting them vertically, were prepared. To separate the mineral particles for the analysis, particles of each part were carefully collected with a knife while magnifying and observing the blackened surface and inner parts for each color using a loupe.

An optical microscope (AXIO Imager A2m, Zeiss, Germany) was used to observe the blackening trend of the colored parts in the cross-sectional specimens. In addition, the carbon content analyzed using an automatic trace element analyzer (Truspec Micro, LECO Corp., St. Joseph, MI, USA) reflected the results of previous studies [36,41].

Bulk powder samples were grounded in an agate mortar to identify major minerals. Furthermore, clay-sized particles were separated to identify traces of clay minerals and iron oxides in the raw material soil constituting the pottery as follows. After adding 2 mL of 5% Na/phosphate as a diffusion agent, approximately 200 mg of the powder collected from each part of the pottery was mixed with 20 mL of distilled water and stored for 12 h. The diffused mixture of specimens was dispersed for 5 min by probe ultrasonication (VC750, Sonics & Materials Inc., Newtown, CT, USA). Then, after precipitating for 40 s, the silt and clay particles remaining in the supernatant were separated. The probe ultrasonication was supplied with a pulse for a total of 10 s at a strength of 0.55 mL/W. After precipitating the separated silt and clay mixture solution in a long-necked plastic tube for 12 h, the separated supernatant was collected again and centrifuged at 7500 rpm to collect the clay particles. The ratio of sample-to-distilled water and the method for dispersing particles used were described in Cho et al. [42] and Lee et al. [43], respectively.

The X-ray diffraction (XRD) analysis was performed using an XRD analyzer (D8 Advanced A25, Bruker, Billerica, MA, USA) operated by the Department of Geological Science, Gyeongsang National University, to identify major minerals, including clay minerals. For the analysis conditions, the scanning interval was set to 0.02° (2θ) at 40 kV and 40 mA. The scanning interval was set to 5–60° (2θ) when analyzing the bulk powder to investigate the major mineral composition with a randomly oriented specimen mounted on a zero-background silicon holder. In the case of clay mineral composition, a region of 5–30° (2θ) was scanned with air-dried preferred orientation specimens on a slide glass. Furthermore, the oriented clay specimens were saturated with ethylene glycol for more than 12 h in order to identify expansible minerals and then used in the analysis [42]. To identify iron oxides, an XRD analyzer (EMPYREAN, Pananalytical, Almelo, the Netherlands) operated by the National Research Institute of Cultural Heritage was used to scan a region of 30–40° (2θ) in a scanning interval of 0.02° (2θ) at conditions of 45 kV, 40 mA. The scanning time was flexibly applied to each specimen to obtain an appropriate diffraction strength for structural analysis with the oriented clay particles on a zero-background silicon plate.

3. Results and Discussion

3.1. Blackening Trend and Carbon Content

Figure 2 shows the blackening trend and the carbon content of each fragment [36,41] that was observed in the cross-section. In PN1 and PN2, blackened marginal parts of approximately 1 mm were observed on the surface. In the case of PN1, a fading trend in the direction of the core of a black or grayish black color was observed, and, in the case of PN2, a fading trend in the direction of the brown core was observed. These blackening trends clearly distinguish these two fragments from the BP type, in which a clear boundary is observed between the blackened part and the body part, owing to the direct painting of black raw material on the surface [5–11]. Furthermore, although a certain amount of carbon was detected in their surface parts, it was not found in the inner parts, regardless of the color; this finding implies that, in these types, carbon accumulated on the surface and it did not penetrate the inner body [41,44]. In contrast, PN3 of the BS type showed a soot coating layer of about 2 mm or larger, and the carbon content was approximately 10 times higher, although the concentration of the black color developed on the surface was distinctly lighter compared to the other two fragments (Figures 1 and 2). Furthermore, this fragment was blackened by the surface deposition of soot and inner penetration, and a large amount of carbon was detected in the blackened inner part, unlike the black or grayish black inner part of PN1, where carbon was not detected.
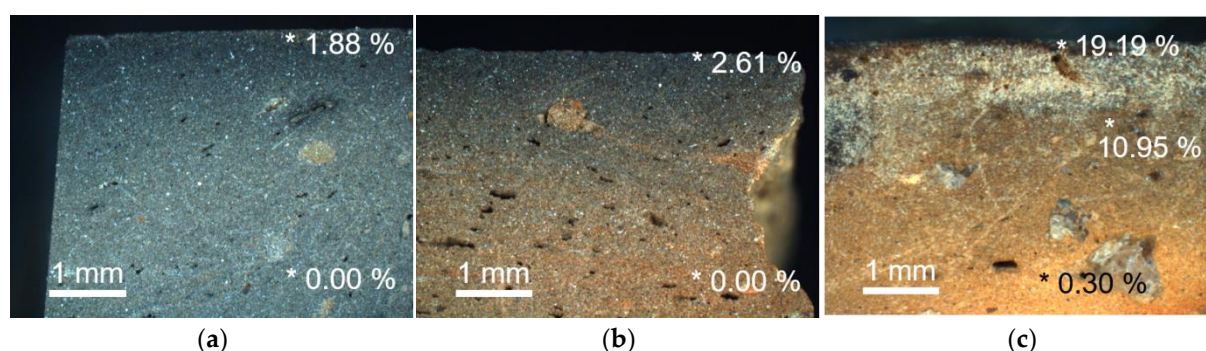

Figure 2. Cross-sectional images of pottery samples: (**a**) PN1, (**b**) PN2, and (**c**) PN3. *: Carbon content figures from previous studies [36,41].

3.2. Major Mineral Composition

Identifying the presence of a certain mineral using XRD is a simple and useful method for assessing the firing temperature of archeological samples produced by heating raw material soil, such as pottery, and it is applied as a reference method in the ceramic archaeothermometry field [44–49]. In the XRD results of the bulk powder samples in this study, the peaks of quartz, plagioclase, alkali feldspar, and mica minerals were recorded without distinction between the surface and the core in every pottery fragment (Figure 3). Feldspar minerals, which started to melt above 1100 °C [47], were detected. Conversely, hercynite, a mineral produced at a temperature of 950 °C or higher, was not detected. Finally, peaks of mica minerals (including illite and muscovite) of weak diffraction intensity were found. These results indicated that all three fragments were produced at a firing temperature of less than 900 °C. This is consistent with the findings of previous research on black pottery from the same site [28].
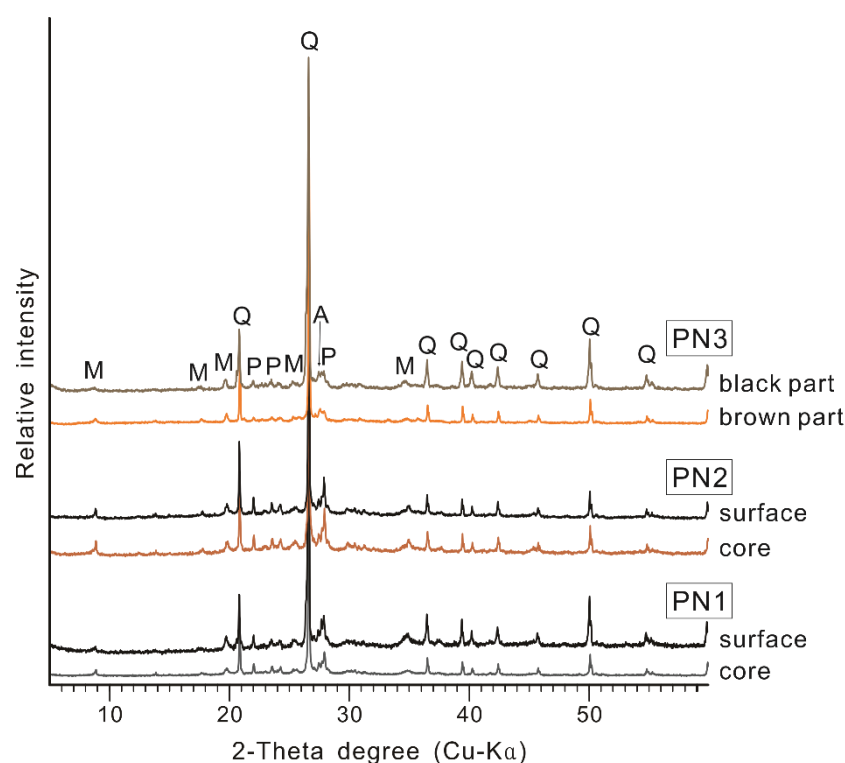
Figure 3. X-ray diffraction patterns of bulk powder samples (A: alkali feldspar, M: mica mineral, P: plagioclase, Q: quartz).

However, in the case of the diffraction patterns of the bulk powder, the peaks of mica are difficult to analyze, as they are present in small amounts due to the higher diffraction intensity of quartz and feldspar. Furthermore, even though the detected minerals were known as white or clear colors, iron oxides—mineralogical factors that induce brownish or blackish colors—were not detected among the soil component materials [6–9,12–21,50–52]. In particular, the iron oxides in the soil exist as nano-sized particles that cover individual soil particles and have low crystallinity—they are almost amorphous in nature [53–59]. To identify such minerals, sorted specimens—prepared by separating and collecting clay particles with a relatively high proportion of iron oxides—must be analyzed.

3.3. Clay Particle XRD and Firing Parameters

In the XRD results of the oriented specimens of the clay particles separated from the pottery, suitable diffraction patterns were recorded to identify clay minerals and iron oxides (Figures 4 and 5). This phenomenon was determined to be due to the relatively distinct decrease in the proportions of quartz and feldspar, while the proportion of clay minerals increased in every specimen since the clay particles were collected. Furthermore, in the case of iron oxides, an identifiable XRD pattern was recorded due to the concentration effect [60] that covered the upper part of the flaky plate, which was predominantly exposed because of the characteristics of the clay mineral particles arranged along the b-axis in the oriented specimens, as shown in Figure 6.
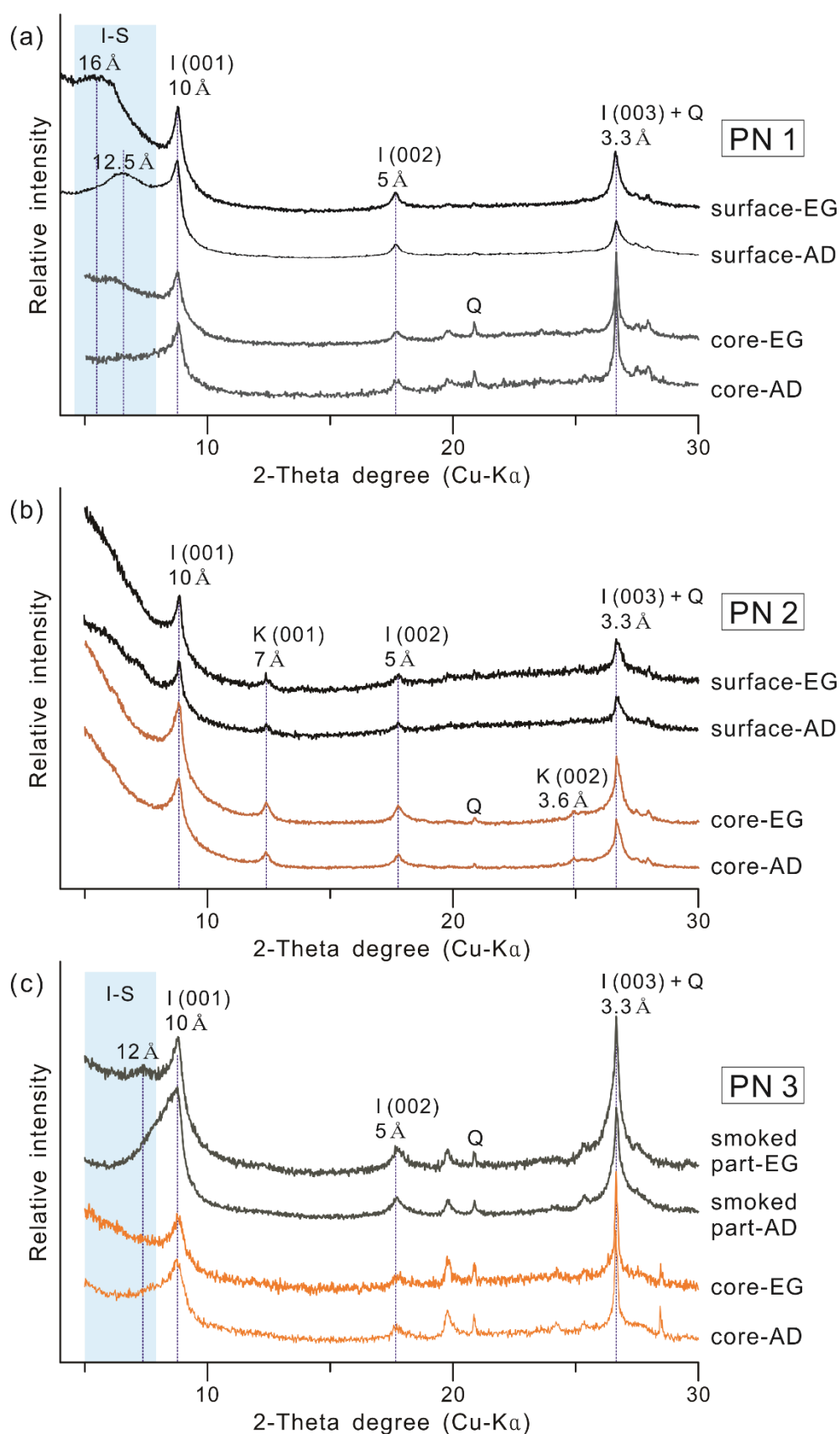
Figure 4. X-ray diffraction patterns of the oriented specimens of clay particles (AD: air-dried, EG: ethylene glycol saturated, I: illite, I–S: illite–smectite mixed layer, K: kaolin, Q: quartz, Blue shaded zone: the diffraction range of the expandable layer by the I–S): (**a**) PN1, (**b**) PN2, and (**c**) PN3.
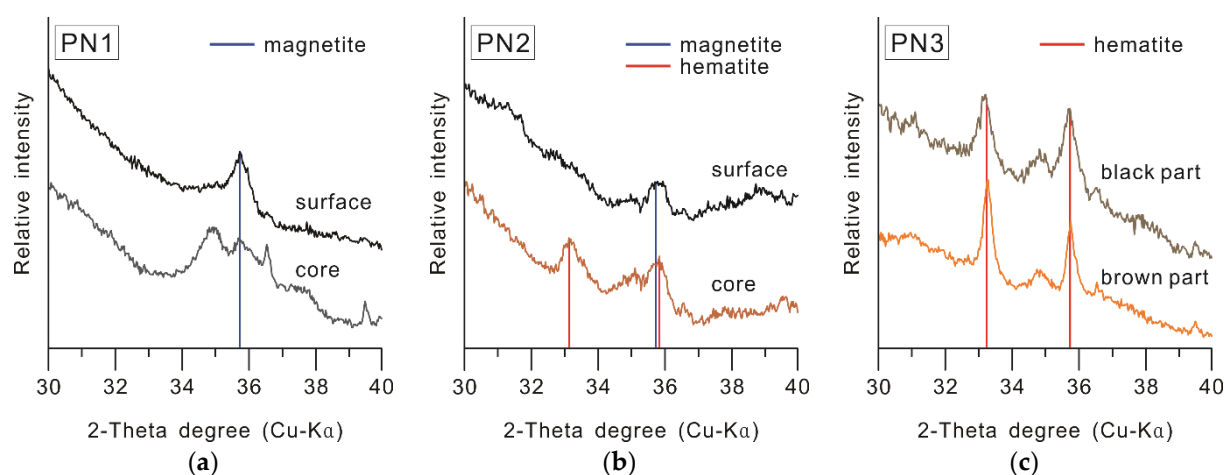
Figure 5. X-ray diffraction patterns with enlarged iron oxide peak area of the oriented samples of clay particles: (**a**) PN1, (**b**) PN2, and (**c**) PN3.
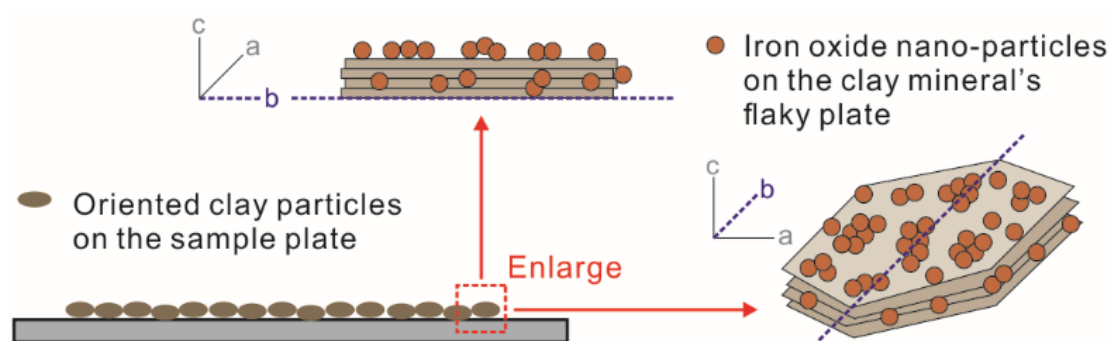

Figure 6. Occurrence types of iron oxide in the clay particles on the preferred orientation specimens.

3.3.1. Clay Mineral Composition

In regards to the clay mineral composition (Figure 4), distinct 10 Å peaks of illite were found in every fragment, and broad peaks of the expandable layer were detected in PN1 and PN3. The presence of an expandable layer is considered to be due to I–S mixed-layer minerals, which indicate rehydration in the poor crystalline illite structure, which occurs in the burial environment [61–63]. Consequently, based on the accurate verification of illite (including other micaceous minerals), which recorded a weak diffraction strength in the XRD results of the bulk powder (Figure 3), the firing temperature of all the fragments was considered to not have exceeded 900 °C [28,44–46]. Furthermore, the presence of the kaolin mineral was confirmed in PN2, the fragment with a brown core. Kaolin is a clay mineral, and its structure is destroyed when heated above 550 °C [52,64,65]. Consequently, PN2, in which the kaolin mineral was detected, was produced at a firing temperature of less than 550 °C, which falls short of the firing temperature range of 700–900 °C estimated in a previous study on black pottery unearthed from the same site [27,28].

3.3.2. Iron Oxide Composition

As shown in Figure 5, the presence of magnetite on the black surfaces of both PN1 and PN2 was confirmed. In the case of the core, relatively weak magnetite peaks were recorded in the black or grayish black core of PN1. In contrast, hematite was detected in the brownish core of PN2. In the case of PN3, which was covered with soot, hematite was detected in both the black-smoked and reddish brown parts.

According to studies on the color change of raw material soil depending on the firing environment [66–69], the composition of iron oxides covering the soil particles is one of the main color development factors. In this regard, the pottery produced by firing in an

oxidation environment shows a red color, along with an increase in the percentage of Fe^{3+} due to the conversion into hematite; in the case of reduction firing, Fe^{2+} increases, showing a black color due to the conversion into magnetite. Based on these results, PN1 and PN2—in which magnetite was detected in the blackened parts—were classified as RB-type pottery, and PN3, in which only hematite was detected, was classified as BP-type pottery, fired in an oxidizing environment. The iron oxide composition for each type of black pottery is consistent with the Mössbauer spectroscopy results of black pottery from the same site [36], and with the properties of the RB pottery reported from various cultural spheres [12–21,66–69]. This finding implies that, in the ancient Baekje period, not only were the BP and BS types produced, as reported previously [27,28,30–35], but the RB type was also produced.

3.4. Manufacturing Techniques for Each Type of Black Pottery

According to the blackened trend (Figure 2), clay mineral composition (Figure 4), and iron oxide composition (Figure 5) observed in the studied ancient Baekje black pottery, the firing technique applied while manufacturing each fragment can be estimated, as shown below [12–21,36,52,64–75]:

- PN1: It is a type of black pottery with a black or grayish black core, in which carbon was not detected. It was estimated to have been produced by reduction firing in the temperature range of 550–900 °C, and it was suggested that the blackening occurred due to the conversion of iron oxides into magnetite in the raw material soil. Furthermore, dark blackening was predicted to have occurred, even in the inner part, through firing in a stronger reduction environment (e.g., higher temperature, reduction gas amount, and reaction duration time) compared to PN2, in which the inner part is brown.

- PN2: It is a type of black pottery in which the core is brown, and a black margin of about 1 mm from the surface has been formed. Since kaolin was detected in both the black surface and the brown core, the result revealed that it was produced by firing at temperatures below 550 °C. Moreover, the study found that it was produced in a reduction firing environment of at least 500 °C, based on the iron oxide composition of the black surface, in which magnetite was detected [76], unlike the brown core, in which hematite was detected. In other words, PN2 was produced by reduction firing in the range of 500–550 °C, and the core seems to have not blackened because it was manufactured at a lower reduction firing condition compared to PN1.

- PN3: The carbon content is distinctly high in the parts where the blackening occurred because of the covering layer of soot. Irrespective of the color in each part, hematite was detected, while kaolin was not. This implies that, in this type, the deposition and penetration of black carbon particles were achieved through firing in a state of contact with vegetable raw material, in an oxidizing environment with temperatures in the range of 550–900 °C.

4. Conclusions

This study attempted to identify clay minerals and iron oxides through XRD analysis of the specimens prepared by separating clay particles from the powder samples of black pottery unearthed from Pungnaptoseong, which is a historical site of the ancient Baekje.

As a result, RB pottery was confirmed to have been produced in the ancient Baekje period through the presence of magnetite detected from the blackened parts of PN1 and PN2, which is clearly distinct from the iron oxide composition of the BS type (PN3)—in which hematite was detected in the blackened parts. Furthermore, the presence of kaolin minerals detected in PN2 indicates firing at temperatures below 550 °C, which confirms the existence of a new category, produced at a lower firing temperature compared to what was learned in the previous studies on Baekje pottery.

Among RB pottery, PN1 shows blackening from the surface to the margin and the core, and the detection of illite and magnetite indicates that it was produced in a reduction

firing environment of 550–900 °C. Furthermore, in the case of PN2, the presence of kaolin with illite was confirmed, and magnetite was detected in the blackened surface and margin, whereas hematite was detected in the core. This finding implies that it was produced through reduction firing at the relatively lower temperature of 500–550 °C.

As described above, through the XRD analysis of the samples of separated clay particles, the composition of clay minerals and iron oxides, which were difficult to identify in the bulk powder XRD, was identified. This information can be used to analyze the firing techniques of pottery. In the future, this analysis method is expected to be used as a simple, precise, and useful mineralogical method for pottery manufacturing techniques, through cross-validation with other analysis methods related to iron oxide composition, along with applying it to various types of pottery.

References

1. Branfman, S. *Raku: A Practical Approach*; Krause Publications: Iola, WI, USA, 2001; p. 176.
2. Watkins, J.C.; Wandless, P.A. *Alternative Kilns and Firing Techniques*; Lark crafts: Asheville, NC, USA, 2006; p. 128.
3. Lazo, E. *Naked Raku and Related Bare Clay Techniques*; American Ceramic Society: Westerville, OH, USA, 2012; p. 151.
4. Dassow, S.V. *Low-Firing and Burnishing*; A & C Black publishers LTD: London, UK, 2013; p. 112.
5. Trąbska, J.; Wesełucha-Birczyńska, A.; Zięba-Palus, J.; Thagård Runge, M. Black painted pottery, Kildehuse II, Odense County, Denmark. *Spectrochim. Acta A Mol. Biomol. Spectrosc.* **2011**, *79*, 824–830. [CrossRef] [PubMed]
6. Hawley, F.M. Prehistoric pottery pigments in the Southwest. *Am. Anthropol.* **1929**, *31*, 731–754. [CrossRef]
7. Stewart, J.D.; Adams, K.R. Evaluating visual criteria for identifying carbon- and iron-based pottery paints from the four corners region using SEM-EDS. *Am. Antiq.* **1999**, *64*, 675–696. [CrossRef]
8. Pendleton, M.; Washburn, D.K.; Ellis, E.A.; Pendleton, B.B. Distinguishing between mineral paint and carbon paint on ancestral Puebloan pottery. *Micros. Today* **2012**, *20*, 32–36. [CrossRef]
9. Pendleton, M.; Washburn, D.K.; Ellis, E.A.; Pendleton, B.B. Comparing the detection of iron-based pottery pigment on a carbon-coated sherd by SEM-EDS and by Micro-XRF-SEM. *Yale J. Biol. Med.* **2014**, *87*, 15–20.
10. Spataro, M.; Cubas, M.; Craig, O.E.; Chapman, J.C.; Boroneant, A.; Bonsall, C. Production and function of Neolithic black-painted pottery from Schela Cladovei (Iron Gates, Romania). *Archaeol. Anthropol. Sci.* **2019**, *11*, 6287–6304. [CrossRef]
11. Rosado, L.; Pevenage, J.V.; Vandenabeele, P.; Candeias, A.; Lopes, M.D.C.; Tavares, D.; Alfenim, R.; Schiavon, N.; Mirao, J. Multi-analytical study of ceramic pigments application in the study of Iron Age decorated pottery from SW Iberia. *Measurement* **2017**, *118*, 262–274. [CrossRef]
12. Gangas, N.H.J.; Kostikas, A.; Simopoulos, A.; Vocotopoulou, J. Mössbauer spectroscopy of ancient Greek pottery. *Nature* **1971**, *229*, 485–486. [CrossRef]
13. Kostikas, A.; Simopoulos, A.; Gangas, N.H.J. Mössbauer study of ancient Greek pottery. *J. Phys.* **1974**, *35*, 107–115.
14. Longworth, G.; Warren, S.E. Mössbauer spectroscopy of Greek 'Etruscan' pottery. *Nature* **1975**, *255*, 625–627. [CrossRef]
15. Nagy, S.; Kuzman, E.; Weiszburg, T.; Gyökeres-Tóth, M.; Riedel, M. Oxide transformation during preparation of black pottery in Hungary. *J. Radioanal. Nucl. Chem.* **2000**, *246*, 91–96. [CrossRef]
16. Epossi Ntah, Z.L.; Sobott, R.; Fabbri, B.; Bente, K. Characterization of some archaeological ceramics and clay samples from Zamala—Far-northern part of Cameroon (West Central Africa). *Cerâmica* **2017**, *63*, 413–422. [CrossRef]
17. Noghani, S.; Emami, M. Mineralogical phase transition on sandwich-like structure of clinky pottery from Parthian Period, Iran. *Period. Mineral.* **2014**, *83*, 171–185.

18. Venkatachalapathy, R.; Bakas, T.; Basavaiah, N.; Deenadayalan, K. Mössbauer and mineral magnetic studies on archaeological potteries from Adhichanallur, Tamilnadu, India. *Hyperfine Interact.* **2008**, *186*, 89–98. [CrossRef]
19. Shimada, I.; Häusler, W.; Jakob, M.; Montenegro, J.; Riederer, J.; Wagner, U. Early pottery making in northern coastal Peru. Part IV: Mössbauer study of ceramics from Huaca Sialupe. *Hyperfine Interact.* **2003**, *150*, 125–139. [CrossRef]
20. Bong, W.S.K.; Matsumura, K.; Nakai, I. Firing technologies and raw materials of typical early and middle Bronze Age pottery from Kaman-Kalehöyük; A statistical and chemical analysis. *Anat. Archaeol. Stud.* **2008**, *17*, 295–311.
21. Meirer, F.; Liu, Y.; Pouyet, E.; Fayard, B.; Cotte, M.; Sanchez, C.; Andrews, J.C.; Mehta, A.; Scianu, P. Full-field XANES analysis of Roman ceramics to estimate firing conditions—A novel probe to study hierarchical heterogeneous materials. *J. Anal. At. Spectrom.* **2013**, *28*, 1870–1883. [CrossRef]
22. Tanthanuch, W.; Pattanasiriwisawa, W.; Somphon, W.; Srilomsak, S. Synchrotron Studies of Ban Chiang Ancient Pottery. *Suranaree J. Sci. Technol.* **2011**, *18*, 15–28.
23. Joseph, D. Investigations on Megalithic Pottery Samples by X-ray Emission Spectroscopy (EDXRF and XANES). *Asian J. Adv. Basic Sci.* **2014**, *3*, 60–66.
24. Hormes, J.; Bovenkamp-Langlois, L.; Klysubun, W.; Kizilkaya, O. Calcium X-ray absorption near edge structure (XANES) spectra: A thermometer for the firing temperature of ceramics? *Microchem. J.* **2020**, *154*, 104571. [CrossRef]
25. Sciau, P.; Relaix, S.; Kihn, Y.; Roucau, C. The role of Microstructure, Nanostructure and Composition in the Brilliant Red Slip of Roman Terra Sigillata Pottery from Southern Gaul. *MRS Online Proc. Libr.* **2005**, *852*, 7–12. [CrossRef]
26. Mirguet, C.; Roucau, C.; Sciau, P. Transmission Electron Microscopy a Powerful Means to Investigate the Glazed Coating of Ancient Ceramics. *J. Nano Res.* **2009**, *8*, 141–146. [CrossRef]
27. Choi, S.W.; Lee, N.S.; Lee, J.H.; Lee, H.S.; Chae, S.J. A study on the occurrence of Paekche burnished black pottery and their reproduction. *Rev. Cult. Herit. Stud.* **2001**, *34*, 4–18.
28. Kim, S.K.; Han, M.S.; Nam, S.W.; Jang, S. Manufacturing characteristics of black burnished pottery from Pungnaptoseong, Beakje. *J. Conserv. Sci.* **2017**, *33*, 417–429.
29. Yoon, Y.J. Study on the pre-historic relics along the Geumho River. *Komunhwa Korea Antiq.* **1969**, *5*, 1–22.
30. Kim, S.K. A Study on Material Characteristics and Making Techniques for Black Burnished Pottery from Hanseong Period of Baekje in Ancient Korea. Ph.D. Thesis, Kongju National University, Koongju, Korea, 2020.
31. Han, Y.H. The newly acquired bronze age artifacts of Chinju National Museum (1984–1985). *Yeongnam Archaeol. Rev.* **1986**, *1*, 151–167.
32. Shin, K.S.; Oh, M.M. The production and restoration of Bronze Age polished pottery through experimental archaeology. *J. Kor. Field Archaeol.* **2010**, *8*, 35–80.
33. Nam, S.W. As production technology, the meaning of the black burnished pottery in Baekje Dynasty. *Korean Archaeol.* **2013**, *89*, 94–137.
34. Nam, S.W.; Kim, S.K. Research on the production technology of black-burnished pottery in Baekje period from the perspective of experimental archaeology. *Ann. Baekje* **2015**, *12*, 5–34.
35. Jin, W.S.J. The Developmental Study of Interior Ceramics Which is Using Traditional Smoked Earthenware Techniques. Master's Thesis, Wonkwang University, Iksan, Korea, 2016.
36. Moon, D.H.; Lee, M.S.; Nam, S.W.; Cho, H.G. A Study on Magnetic Properties and Role of the Iron Oxides in Ancient Baekje Black Burnished Pottery by Mössbauer Spectroscopy. *J. Magn.* **2020**, *25*, 496–502. [CrossRef]
37. Biscaye, P.E. Mineralogy and sedimentation of recent deep-sea clay in the Atlantic Ocean and adjacent seas and oceans. *Geol. Soc. Am. Bull.* **1965**, *76*, 803–832. [CrossRef]
38. Lackschewitz, K.S.; Singer, A.; Botz, R.; Garbe-Schönberg, D.; Stoffers, P. Mineralogy and geochemistry of clay minerals near a hydrothermal site in the Escanaba Trough, Gorda Ridge, northeast Pacific Ocean. In Proceedings of the Ocean Drilling Program, Scientific Results; Zierenberg, R.A., Fouquet, Y., Miller, D.J., Normark, W.R., Eds.; Texas A&M University: College Station, TX, USA, 2000; Volume 169, pp. 1–24.
39. Bristow, T.F.; Kennedy, M.J.; Derkowski, A.; Droser, M.L.; Jiang, G.; Creaser, R.A. Mineralogical constraints on the paleoenvironments of the Ediacaran Doushantuo Formation. *Proc. Natl. Acad. Sci. USA* **2009**, *106*, 13190–13195. [CrossRef]
40. Koo, H.J.; Cho, H.G. Changes in detrital sediment supply to the central Yellow Sea since the last deglaciation. *Ocean Sci.* **2020**, *16*, 1247–1259. [CrossRef]
41. Moon, D.H. Mineralogical Study on the Raw Materials of Cultural Properties; Interpretation and Rediscovery. Ph.D. Thesis, Gyeongsang National University, Jinju, Korea, 2021.
42. Cho, H.G.; Kim, S.-O.; Kwak, K.Y.; Choi, H. Clay mineral distribution and provenance in the Heuksan mud belt, Yellow Sea. *Geo-Mar. Lett.* **2015**, *35*, 411–419. [CrossRef]
43. Lee, W.C.; Kim, S.-O.; Kim, Y.H. Characterization of Behavior of Colloidal Zero-Valent Iron and Magnetite in Aqueous Environment. *J. Miner. Soc. Korea* **2015**, *28*, 95–108. [CrossRef]
44. Rice, P.M. *Pottery Analysis: A Sourcebook*, 1st ed.; The University of Chicago Press: Chicago, IL, USA, 1987; p. 559.
45. Quinn, P.S.; Benzonelli, A. X-ray diffraction and archaeological materials analysis. In *The SAS Encyclopedia of Archaeological Sciences*, 1st ed.; López Varela, S.L., Ed.; Wiley Blackwell: Hoboken, NJ, USA, 2018.
46. Viania, A.; Cultrone, G.; Sotiriadisa, K.; Ševčíka, R.; Šašeka, P. The use of mineralogical indicators for the assessment of firing temperature in fired-clay bodies. *Appl. Clay Sci.* **2018**, *163*, 108–118. [CrossRef]
47. Quinn, P.S. *Ceramic Petrography: The Interpretation of Archaeological Pottery and Related Artefacts in Thin Section*, 1st ed.; Archaeopress: Oxford, UK, 2013.

48. Maggetti, M.; Neururer, C.; Ramseyer, D. Temperature evolution inside a pot during experimental surface (bonfire) firing. *Appl. Clay Sci.* **2011**, *53*, 500–508. [CrossRef]
49. Travé Allepuz, E. Colour Transformation and Textural Change in Biotite: Some Remarks for the Interpretation of Firing Technology in Greyware Pottery Thin-Sections. *Minerals* **2021**, *11*, 428. [CrossRef]
50. Middleton, A.P. Technological investigation of the coatings on some 'hematite-coated' pottery from southern England. *Archaeometry* **2007**, *29*, 250–261. [CrossRef]
51. De Bonis, A.; Cultrone, G.; Grifa, C.; Langella, A.; Leone, A.P.; Mercurio, M.; Morra, V. Different shades of red: The complexity of mineralogical and physico-chemical factors influencing the colour of ceramics. *Ceram. Int.* **2017**, *43*, 8065–8074. [CrossRef]
52. Heimann, R.; Franklin, U.M. Archaeo-thermometry: The assessment of firing temperatures of ancient ceramics. *J. Int. Inst. Conserv.-Can. Group* **1980**, *4*, 23–45.
53. Van Diepen, A.M.; Popma, J.A. Mössbauer effect and magnetic properties of an amorphous Fe_2O_3. *J. Phys. Colloq.* **1976**, *37*, 755–758. [CrossRef]
54. Cao, X.; Prozorov, R.; Koltypin, Y.; Kataby, G.; Felner, I.; Gedanken, A. Synthesis of pure amorphous Fe_2O_3. *J. Mater. Sci.* **1997**, *12*, 402–406. [CrossRef]
55. Schneeweiss, O.; Zbořil, R.; David, B.; Heřmánek, M.; Mashlan, M. Solid-state synthesis of α-Fe and iron carbide nanoparticles by thermal treatment of amorphous Fe_2O_3. *Hyperfine Interact.* **2009**, *189*, 167–173. [CrossRef]
56. Topsøe, H.; Dumesic, J.; Boudart, M. Mössbauer spectra of stoichiometric and nonstoichiometric Fe_3O_4 microcrystals. *J. Phys. Colloq.* **1974**, *35*, 411–413. [CrossRef]
57. Koch, C.B.; Jiang, J.Z.; Mørup, S. Mechanical milling of Fe_3O_4/SiO_2: Formation of an amorphous Fe(II)-Si-O-containing phase. *Scr. Mater.* **1999**, *12*, 233–236.
58. Rodriguez, A.F.R.; Coaquira, J.A.H.; Morales, M.A.; Faria, F.S.E.D.V.; Cunha, R.M.; Santos, J.G.; Silveira, L.B.; Candela, D.R.S.; Baggio-Saitovitch, E.M.; Rabelo, D.; et al. Synthesis, characterization and magnetic properties of polymer-Fe_3O_4 nanocomposite. *Spectrochim. Acta. A Mol. Biomol. Spectrosc.* **2013**, *100*, 101–103. [CrossRef]
59. Hah, H.Y. Mössbauer Spectroscopy of Iron Oxide Nanoparticles: Materials for Biomedical Applications. Ph.D. Thesis, University of Tennessee, Knoxville, TN, USA, 2018.
60. Zhang, X.W.; Kong, L.W.; Cui, X.L.; Yin, S. Occurrence characteristics of free iron oxides in soil microstructure: Evidence from XRD, SEM and EDS. *Bull. Eng. Geol. Environ.* **2016**, *75*, 1493–1503. [CrossRef]
61. Maggetti, M. 11. Phase analysis and its significance for technology and origin. In *Archaeological Ceramics*; Olin, J.S., Franklin, A.D., Eds.; Smithsonian Institution Press: Washington, DC, USA, 1982; pp. 121–133.
62. Wilson, M.A.; Hamilton, A.; Ince, C.; Carter, M.A.; Hall, C. Rehydroxylation (RHX) dating of archaeological pottery. *Proc. R. Soc. A* **2012**, *468*, 3476–3493. [CrossRef]
63. Weiner, S.; Nagorsky, A.; Feldman, Y.; Kossay, A. Archaeological Ceramic Diagenesis: Clay Mineral Recrystallization in Sherds from a Late Byzantine Kiln, Israel. *Minerals* **2020**, *10*, 408. [CrossRef]
64. Bellotto, M.; Gualtieri, A.; Artioli, G.; Clark, S.M. Kinetic study of the kaolinite-mullite reaction sequence. Part I: Kaolinite dehydroxylation. *Phys. Chem. Miner.* **1995**, *22*, 207–217. [CrossRef]
65. Murad, E.; Wagner, U. Pure and impure clays and their firing products. *Hyperfine Interact.* **1989**, *45*, 161–177. [CrossRef]
66. Chevalier, R.; Coey, J.M.D.; Bouchez, R. A study of iron in fired clay: Mössbauer effect and magnetic measurement. *J. Phys. Colloq.* **1976**, *37*, 861–865. [CrossRef]
67. Maniatis, Y.; Tite, M.S. Technological examination of Neolithic-Bronze age pottery from central and southeast Europe and from the near East. *J. Archaeol. Sci.* **1981**, *8*, 59–76. [CrossRef]
68. Mackenzie, K.J.D.; Cardile, C.M. A 57Fe Mössbauer study of black coring phenomena in clay-based ceramic materials. *J. Mater. Sci.* **1990**, *25*, 2937–2942. [CrossRef]
69. Maritan, L.; Nodari, L.; Mazzoli, C.; Milano, A.; Russo, U. Influence of firing conditions on ceramic products: Experimental study on clay rich in organic matter. *Applied Clay Sci.* **2006**, *31*, 1–15. [CrossRef]
70. Dawson, D.; Kent, O. Experiments in reduction firing. *Bull. Exp. Firing Grp.* **1987**, *5*, 34–41.
71. Dawson, D.; Kent, O. Reduction fired low-temperature ceramics. *Postmediev. Archaeol.* **1999**, *33*, 164–178. [CrossRef]
72. Thér, R.; Gregor, M. Experimental reconstruction of the pottery firing process of Late Bronze Age pottery from north-eastern Bohemia. In *Archaeological Ceramics: A Review of Current Research*; Scarcella, S., Ed.; Archaeopress: Oxford, UK, 2011; pp. 128–142.
73. Kingery, W.D. Attic Pottery Gloss Technology. *Archaeomaterials* **1991**, *5*, 47–54.
74. Zhushchikhovskaya, I.S.; Nikitin, G. Ceramic firing structures in Prehisoric and ancient societies of the Russian far East. *Asian Perspect.* **2015**, *53*, 121–149. [CrossRef]
75. Heimann, R.B.; Maggetti, M. The struggle between thermodynamics and kinetics: Phase evolution of ancient and historial ceramics. In *EMU Notes in Mineralogy: The Contribution of Mineralogy to Cultural Heritage*; Artioli, G., Oberti, R., Eds.; Mineralogical Society: London, UK, 2019; Volume 20, pp. 233–281.
76. Yu, J.; Han, Y.; Li, Y.; Gao, P.; Li, W. Mechanism and kinetics of the reduction of hematite to magnetite with CO-CO_2 in a micro-fluidized bed. *Minerals* **2017**, *7*, 209. [CrossRef]